

ORIGINAL PAPER

Kentaro Okamura · Kinji Asahina · Hiroaki Fujimori · Rie Ozeki · Keiko

Shimizu-Saito · Yujiro Tanaka · Kenichi Teramoto · Shigeki Arii · Kozo

Takase · Miho Kataoka · Yoshinori Soeno · Chise Tateno · Katsutoshi

Yoshizato · Hirobumi Teraoka

**Title: Generation of hybrid hepatocytes by cell fusion from monkey embryoid
body cells in the injured mouse liver**

K. Okamura · K. Asahina · H. Fujimori · R. Ozeki · K. Shimizu-Saito · H.

Teraoka

Department of Pathological Biochemistry, Medical Research Institute, Tokyo Medical
and Dental University, Tokyo, Japan

Y. Tanaka · K. Teramoto · S. Arii · K. Takase

Graduate School of Medicine and Dentistry, Tokyo Medical and Dental University,
Tokyo, Japan

M. Kataoka · Y. Soeno · C. Tateno · K. Yoshizato

Yoshizato Project, CLUSTER, Prefectural Institute of Industrial Science and
Technology, Hiroshima, Japan

Y. Soeno

PhoenixBio Co., Ltd. Hiroshima, Japan

K. Yoshizato

Developmental Biology Laboratory, Department of Biological Science, Graduate
School of Science, Hiroshima University, Hiroshima, Japan

Correspondence: K. Asahina

Department of Pathological Biochemistry, Medical Research Institute, Tokyo Medical
and Dental University, 2-3-10 Kandasurugadai, Chiyoda-ku, Tokyo 101-0062, Japan

e-mail: asahina.pbc@mri.tmd.ac.jp

Tel: 81-3-5280-8076

Fax: 81-3-5280-8075

Abstract

Monkey embryonic stem (ES) cells have characteristics that are similar to human ES cells, and might be useful as a substitute model for preclinical research. When embryoid bodies (EBs) formed from monkey ES cells were cultured, expression of many hepatocyte-related genes including cytochrome P450 (Cyp) 3a and Cyp7a1 was observed. Hepatocytes were immunocytochemically observed using antibodies against albumin, cytokeratin-8/18, and α 1-antitrypsin in the developing EBs. The in vitro differentiation potential of monkey ES cells into the hepatic lineage prompted us to examine the transplantability of monkey EB cells. As an initial approach to assess the repopulation potential, we transplanted EB cells into immunodeficient urokinase-type plasminogen activator transgenic mice that undergo liver failure. After transplantation, the hepatocyte colonies expressing monkey albumin were observed in the mouse liver. Fluorescence in situ hybridization revealed that the repopulating hepatocytes arise from cell fusion between transplanted monkey EB cells and recipient mouse hepatocytes. In contrast, neither cell fusion nor repopulation of hepatocytes was observed in the recipient liver after undifferentiated ES cell transplantation. These results indicate that the differentiated cells in developing monkey EBs, but not contaminating ES cells, generate functional hepatocytes by cell fusion with recipient mouse hepatocytes, and repopulate injured mouse liver.

Key Words: Cynomolgus · Embryonic stem cells · Hepatocyte differentiation · Transgenic mouse · Xenogeneic transplantation

Introduction

Mouse embryonic stem (ES) cells established from the inner cell mass of blastocysts are capable of differentiating into three embryonic germ layers and germ cells (Evans and Kaufman 1981; Martin 1981). When ES cells are allowed to aggregate in suspension culture, they form structures termed embryoid bodies (EBs) that resemble embryos at the egg-cylinder stage. EBs can differentiate into multiple cell types, such as hematopoietic cells, cardiac muscle, and neurons *in vitro* (Doetschman et al. 1985). Hepatic differentiation from mouse ES cells has been reported *in vitro* and/or *in vivo* (Hamazaki et al. 2001; Chinzei et al. 2002; Jones et al. 2002; Yamada et al. 2002; Yamamoto et al. 2003; Asahina et al. 2004; Jochheim et al. 2004). Previously, we showed that cultured EBs derived from mouse ES cells express hepatocyte-related genes including albumin (Alb), α -fetoprotein (Afp), and cytochrome P450 (Cyp) 7a1 (Chinzei et al. 2002; Asahina et al. 2004). Furthermore, a transplantation experiment revealed that the cells derived from EBs can integrate into the recipient parenchyma and synthesize ALB (Chinzei et al. 2002; Kumashiro et al. 2005).

ES cell lines have also been established from the inner cell mass of monkey and human blastocysts (Thomson et al. 1998; Reubinoff et al. 2000; Suemori et al. 2001). The phenotype of human ES cells is known to be similar to that of monkey ES cells but differs from that of mouse ES cells with regard to morphology, response to leukemia inhibitory factor (LIF), and gene expression patterns (Thomson et al. 1998; Reubinoff et al. 2000; Suemori et al. 2001; Ginis et al. 2004). Differentiation of hepatocyte-like cells

from human ES cells has also been reported (Itskovitz-Eldor 2000; Rambhatla et al. 2003; Lavon et al. 2004). Although human ES cells are expected as an unlimited source for cell replacement therapy, artificial liver devices, and in vitro drug tests (Ohashi et al. 2001; Strain and Neuberger 2002; Brandon et al. 2003), its use for basic and clinical researches has been regulated in many countries because of bioethical issues. Thus, monkey ES cells might be useful as a substitute model for preclinical research using human ES cells (Suemori et al. 2001).

In the present study, we showed the differentiation potential of monkey ES cells into the hepatic lineage in vitro. As an initial approach to assess the repopulation potential of ES-derived hepatocytes in the liver, we transplanted disaggregated monkey EB cells into immunodeficient urokinase-type plasminogen activator (uPA) transgenic mice. The transgenic mice expressing uPA in the hepatocytes result in liver injury and undergo hypofibrinogenemia (Sandgren et al. 1991). It has been reported that transplanted hepatocytes selectively repopulate and form nodules in the recipient uPA mouse liver (Rhim et al. 1994). In addition, crossing the uPA mice to immunodeficient mice allowed us to transplant xenogeneic hepatocytes including rats and humans (Rhim et al. 1995; Dandri et al. 2001; Mercer et al. 2001; Strick-Marchand et al. 2004; Tateno et al. 2004). Xenogeneic transplantation revealed that the monkey EB-derived cells repopulate in the recipient mouse parenchyma and synthesize ALB. Fluorescence in situ hybridization (FISH) demonstrated that the repopulated hepatocytes arise from cell fusion between monkey EB cells and mouse hepatocytes in the liver.

Materials and methods

Culture of ES cells

Cynomolgus (*Macaca fascicularis*) monkey ES cells (CMK6) were obtained from Asahi Techno Glass (Chiba, Japan) (Suemori et al. 2001). Undifferentiated ES cells were maintained on a feeder layer of mitomycin C-treated mouse embryonic fibroblasts in an ES medium consisting of a 1:1 mixture of Dulbecco's modified Eagle's medium and Ham's nutrient mixture F-12 (Sigma, St. Louis, MO, USA), 20% Knockout SR (KSR), a chemically defined formulation (Invitrogen, Carlsbad, CA, USA), 2 mM L-glutamine, 1% non-essential amino acids, 0.1 mM 2-mercaptoethanol, 1 mM sodium pyruvate, 100 U/ml penicillin, and 100 µg/ml streptomycin.

Differentiation of ES cells

ES cells were suspended in a differentiation medium consisting of the ES medium supplemented with 20% fetal bovine serum (FBS; JRH Biosciences, Lenaxa, KS, USA) instead of KSR. ES cells were cultured for 2 days using the hanging drop culture method (3×10^3 cells per 30 µl in each drop) (Chinzei et al. 2002). The EBs formed in the drops were plated on culture dishes.

Cloning of Cynomolgus cDNAs

Total RNA was extracted from an adult female cynomolgus monkey (20 years of age)

liver using an RNeasy Kit (Qiagen, Valencia, CA, USA). cDNAs were synthesized using 1 µg of total RNA, Superscript II, and oligo (dT) primers (Invitrogen) according to the manufacturer's instructions. cDNAs of cynomolgus Alb, Afp, ornithine transcarbamylase (Otc), carbamoyl-phosphate synthetase 1 (Cps1), Cyp7a1, Oct-3/4, and β-actin were cloned using RT-PCR with primers for the corresponding human genes (Table 1). The PCR products were subcloned into a PCR-TOPO vector (Invitrogen) and sequenced. Cynomolgus Alb (GenBank accession number: AB158629), Afp (AB158630), Otc (AB159732), Cps1 (AB159731), Cyp7a1 (AB211232), Oct-3/4 (AB218422), and β-actin (AB159730) cDNAs have a similarity of 96.4%, 97.8%, 96.3%, 98.9%, 97.7%, 97.6%, and 96.4%, respectively, to the corresponding human cDNAs.

RT-PCR analysis

cDNAs were synthesized as described above. PCR was performed using FastStart Taq DNA polymerase (Roche Diagnostics, Penzberg, Germany) under the following conditions: 94°C for 10 min followed by 25 to 35 cycles of denaturing at 94°C for 45 sec, annealing at 60°C for 45 sec, and extension at 72°C for 45 sec, followed by a final extension for 8 min at 72°C. The PCR primers, cycles, and amplified size for each gene are listed in Table 1. The primers were designed from putative different exons that were aligned with the human genome DNA sequence for each gene.

Real-time RT-PCR

Monkey ES cells and EBs at culture day 25 were treated with 50 μ M rifampicin (Sigma) for 48 h. cDNAs were synthesized and amplified using a Quantitest SYBR Green PCR Kit (Qiagen) and a Light Cycler (Roche Diagnostics) according to the manufacturer's instructions. A series of diluted plasmid cDNAs containing each gene was used to make the standard amplification curves. The mRNA copy numbers in the cDNA samples were then calculated using the standard amplification curves. The expression of Cyp3a in each sample was normalized based on the expression of β -actin.

Immunocytochemistry

EBs were fixed with 80% acetone for 20 min at -20°C . The cells were then blocked with 0.02% goat sera, incubated with 200-fold diluted rabbit anti-human ALB antibodies (DakoCytomation, Glostrup, Denmark) or rabbit anti-human α 1-antitrypsin (AAT) antibodies (DakoCytomation) for 1 h, and incubated with 200-fold diluted Alexa Fluor 555-labeled goat anti-rabbit IgG antibodies (Molecular Probes, Eugene, OR, USA) for 30 min. For double immunostaining, the samples were incubated with 20-fold diluted mouse anti-human cytokeratin-8/18 (CK8/18) antibodies (ICN Pharmaceuticals, Aurora, OH, USA) for 1 h, and incubated with 200-fold diluted fluorescein isothiocyanate (FITC)-labeled goat anti-mouse IgG antibodies (Sigma) for 30 min. Nuclei were stained with DAPI II counterstain (Vysis, Downers Grove, IL, USA). The samples were observed with a fluorescence microscope.

Transplantation of monkey ES cells and EB cells into uPA^{+/-}/SCID^{+/+} mice

We crossed transgenic mice carrying uPA gene linked to the Alb enhancer/promoter {B6SJL-TgN (Alb1Plau)144Bri, the Jackson Laboratory} (Sandgren et al. 1991) with severe combined immunodeficient (SCID) mice (Fox Chased SCID C.B-17/Icr.SCID Jcl, Clea Japan, Inc.). Genotypes of uPA and SCID were determined as previously described (Tateno et al. 2004). uPA^{+/-}/SCID^{+/+} mice were intraperitoneally injected with 100 µl of 1 mg/ml anti-asialo GM1 rabbit antiserum (Wako, Osaka, Japan) 1 day before transplantation. To prepare disaggregated cells, monkey ES cells and EBs at day 21 were treated with trypsin-EDTA. The 2- to 3-week-old mice were anesthetized with ether and injected with 5-7.5 x 10⁵ monkey ES cells or EB cells through a small left-flank incision into the inferior splenic pole. The lower reaches of the injection site were tied with string for hemostasis. These experiments were approved by the ethics board of the Hiroshima Prefectural Institute of Industrial Science and Technology. Blood samples were collected and the level of monkey ALB was determined by enzyme-linked immunosorbent assay (ELISA) with Albuwell (Exocell, Philadelphia, PA, USA) for human ALB. Teratoma formation in the recipient livers was examined 3 weeks after transplantation. Each recipient liver was photographed, and the area of red-colored nodules in the recipient liver was quantified with an Image J software. The proportion of the red-colored nodules was calculated as the ratio of the red-colored nodule area to the entire area of the recipient liver.

Genomic in situ hybridization and immunohistochemistry

The livers were fixed with formalin and embedded in paraffin. Liver sections (10 μm) were prepared from 3 liver pieces of each of 6 recipient mice. The sections were deparaffinized in xylene and incubated in 10 mM Na-citrate buffer (pH 6.0) at 95 °C for 40 min. The sections were treated with 0.3% hydrogen peroxide for 20 min and digested with 1 $\mu\text{g}/\text{ml}$ proteinase K for 10 min at 37 °C. The DNA in the sections was denatured for 6 min at 90 °C, and the sections were hybridized with biotinylated human DNA probes (DakoCytomation) for 2 h at 37 °C (Tateno et al. 2004). The probes were detected using a GenPoint system (DakoCytomation) according to manufacture's instruction. Briefly, the sections were washed with a stringent wash solution, incubated with horseradish peroxidase (HRP)-conjugated streptavidin. After washing, the sections were incubated with biotin-conjugated tyramide, and then treated with HRP-conjugated streptavidin. The hybridized probes were visualized with diaminobenzidine. After hybridization, sections were blocked with 0.02% goat sera, incubated with 100-fold diluted rabbit anti-human ALB antibodies for 30 min, and incubated with 200-fold diluted Alexa Fluor 555-labeled anti-rabbit IgG antibodies for 30 min. After in situ hybridization, the liver sections were photographed, and the area of the human DNA probe-positive cells was quantified with an Image J software. The percentage of the monkey-derived cells in the recipient liver was estimated as the ratio of the area occupied by human DNA-positive cells to the entire area examined in the in situ

hybridization sections.

Double FISH for monkey and mouse chromosomes

Double FISH for the monkey and mouse genomic DNA was performed. After the digestion with proteinase K, the liver sections were treated with 10 µg/ml RNaseA (Sigma) for 30 min at 37 °C, and then hybridized with the biotinylated human DNA probes and FITC-labeled mouse pan-centromeric chromosome paint probes (Cambio, Cambridge, UK) for 16 h at 37 °C. The hybridized human DNA probes were detected with HRP-conjugated streptavidin, biotin-conjugated tyramide, and tetramethylrhodamine isothiocyanate-conjugated extravidin (Sigma). The resulting signals were observed with a fluorescence microscope.

Results

Expression of hepatocyte-related genes in cultured EBs

To address the differentiation potential of monkey ES cells into hepatic lineage, EBs were formed from monkey ES cells by the hanging drop culture, and then cultured on dishes. RT-PCR showed that Alb mRNA, which is a marker for hepatocytes, was expressed in developing EBs from culture day 14 onwards (Fig. 1A). The expression of Afp, which is a marker of visceral endoderm and fetal hepatocytes, was detected from culture day 3 and maintained thereafter, whereas the expression of Alb and Afp was not

observed in the ES cells (Fig. 1A). The expression of *Otc* and *Cps1*, which are involved in urea synthesis, was weakly detected in ES cells, and up-regulated on culture day 7 and day 3, respectively. *Cyp7a1* encoding cholesterol 7 α -hydroxylase, which is specifically expressed in mouse hepatocytes but not in the visceral endoderm (Asahina et al. 2004), was detected from culture day 3. The expression of Oct-3/4, a marker for ES cells, decreased with the differentiation of the EBs. CYP3A is capable of metabolizing about half of the clinically used drugs in human hepatocytes, and its expression is known to be induced by rifampicin (Rae et al. 2001). Quantitative real-time RT-PCR revealed that rifampicin caused a 2-fold induction in *Cyp3a* mRNA in the EBs (Fig. 1B). No expression was detected in undifferentiated ES cells (Fig. 1B) and HepG2 cells (data not shown). These expression profiles suggest that monkey ES cells have differentiation potential into the hepatic lineage in vitro.

Immunocytochemistry of hepatic markers

To confirm the differentiation of hepatocytes, we performed immunocytochemical analysis on day 21 EBs using antibodies against ALB, CK8/18, and AAT that are markers for hepatocytes. Morphologically distinct cell types migrated away from the attached EBs cultured at day 21 (Fig. 2A). Immunocytochemistry showed that EBs contained ALB-positive cells (Fig. 2B). Almost all ALB-expressing cells were also stained with anti-CK8/18 antibodies (Fig. 2C, D). The double positive cells were estimated to be about 5% in the developing EBs. No signals were observed without the

anti-ALB antibodies (Fig. 2E). AAT-expressing cells were also positive for anti-CK8/18 antibodies (Fig. 2F-H).

Transplantation of monkey EB cells into uPA^{+/-}/SCID^{+/+} mice

The above in vitro experiments prompted us to examine the transplantability of the ES-derived hepatocytes. However, lack of monkey hepatocyte specific antibodies hampered isolation of hepatocytes from cultured EBs. As an initial approach to assess the repopulation potential of ES-derived hepatocytes in the liver, disaggregated monkey EB cells cultured for 21 days were transplanted into 6 uPA^{+/-}/SCID^{+/+} mice.

Two-week-old uPA^{+/-}/SCID^{+/+} mouse liver remains white-colored due to hepatic injury, and red foci derived from the transgene-deficient hepatocytes are sparsely seen in the white-colored liver (Fig. 3A) (Sandgren et al. 1991). Fig. 3B shows a representative (Exp. 1, #1) of the uPA^{+/-}/SCID^{+/+} liver 3 weeks after transplantation of monkey EB cells. Red-colored nodules possibly derived from transplanted monkey cells and/or recovered recipient hepatocytes, in which the uPA transgenes were deleted, appeared in the uPA^{+/-}/SCID^{+/+} livers. The average proportion of the red-colored nodule was 28.8% in 5 recipient mouse livers (Table 2). Teratoma was observed neither in liver nor in spleen of all mice.

Detection of monkey ES-derived hepatocytes in mouse liver

In order to detect donor monkey cells in mouse liver, we tested the validity of human

genomic DNA probes and anti-human specific ALB antibodies on monkey liver sections. Previously, we detected human hepatocytes in chimeric mouse liver using the human genomic DNA probes by genomic in situ hybridization (Tateno et al. 2004). Genomic in situ hybridization revealed that 43% nuclei of monkey liver cells were positive for the human genomic DNA probes because of the partial sampling of hepatocyte nuclei in the tissue sections (Fig. 3C). No signals were detected in uPA^{+/-}/SCID^{+/+} mouse liver (Fig. 3D), indicating the validity of genomic in situ hybridization using the human probes on monkey cells. Furthermore, immunohistochemistry showed that the anti-human specific ALB antibodies react with monkey hepatocytes (Fig. 3E), but not with uPA^{+/-}/SCID^{+/+} mouse hepatocytes (Fig. 3F).

Three weeks after transplantation of monkey EB cells, we collected the red-colored nodules from the 3 uPA^{+/-}/SCID^{+/+} mouse livers and were examined by in situ hybridization with human DNA probes (Table 2, Exp. 1). Clusters consisting of positive nuclei for the human DNA probes were detected in the recipient mouse liver (Fig. 3G, I). Immunohistochemistry showed that the human DNA probe-positive cells, but not recipient mouse hepatocytes, are positive for the human specific ALB antibodies (Fig. 3G-J). The percentage of monkey-derived cells in the red-colored nodules of the recipient liver was estimated as the ratio of the area occupied by human DNA-positive cells to the entire red-colored nodule area examined in the in situ hybridization sections. The average percentage of monkey-derived cells was 18.6% in the red-colored nodules of three mouse livers (Table 2, Exp. 1). The percentage of monkey-derived cells was

ranged from 1.5% to 15.8% in the whole mouse livers (Table 2, Exp. 1). We also examined the entire liver containing red- and white-colored nodules of each 3 uPA^{+/-}/SCID^{+/+} mouse (Table 2, Exp. 2). The percentage of monkey-derived cells is ranged from 0.5% to 13.6% in the entire mouse livers (Table 2). Thus, the average monkey-derived cell contribution was 7.4% in the recipient liver.

Monkey ALB in the recipient mouse sera (Exp. 2, #1-3) was measured with an ELISA kit for human ALB. The concentration of normal monkey serum was measured as 75.3 µg/ml, and no monkey ALB was detected in the control uPA^{+/-}/SCID^{+/+} mouse serum. The monkey ALB level in the sera of three transplanted mice was 1.26 ± 0.24 µg/ml. These results indicate that monkey ES-derived hepatocytes are functional in the recipient mouse liver.

Cell fusion between monkey EB cells and recipient mouse hepatocytes

As observed in Fig. 3I, the nuclei in monkey EB-derived hepatocytes were larger than those in recipient hepatocytes in the uPA^{+/-}/SCID^{+/+} mouse, implying that the hepatocytes result from cellular polyploidization or cell fusion. To determine whether the repopulating hepatocytes result from integration of monkey EB-derived hepatocytes or from cell fusion between monkey and mouse cells, we performed double FISH analysis on the liver sections using the human DNA probes and mouse pan-centromeric probes. Double FISH analysis revealed that the nuclei of the control monkey liver section were hybridized with human DNA probes (Fig. 4A), but not with the mouse

probes (Fig. 4B). In contrast, the nuclei of the control mouse liver were hybridized with the mouse probes (Fig. 4D), but not with human probes (Fig. 4C), indicating the validity of these probes.

Three weeks after transplantation, the cluster of hepatocytes containing monkey chromosomes was detected using the human DNA probes in the recipient uPA^{+/-}/SCID^{+/+} mouse liver (Fig. 4E). Surprisingly, these hepatocytes were also hybridized with mouse DNA probes (Fig. 4F, G). The large nuclei of the hepatocytes were clearly hybridized with both human and mouse DNA probes (Fig. 4H). On the same section, there were recipient uPA^{+/-}/SCID^{+/+} mouse hepatocytes positive for the mouse probes (Fig. 4J), but not for the human probes (Fig. 4I). Hepatocyte colonies containing nuclei hybridized with only human probes were not detected in the transplanted uPA^{+/-}/SCID^{+/+} mouse liver. From these results, we concluded that the repopulating hepatocytes arise from cell fusion between transplanted monkey cells and recipient mouse hepatocytes in the uPA^{+/-}/SCID^{+/+} mouse liver.

ES cells were not responsible for the cell fusion with recipient hepatocytes

It has been reported that mouse undifferentiated ES cells fuse with mouse bone marrow cells and neural stem cells in vitro (Terada et al. 2002; Ying et al. 2002), implying that residual ES cells in the cultured EBs generate the hybrid hepatocytes by cell fusion in the mouse liver. In order to assess the possibility, we transplanted undifferentiated monkey ES cells into uPA^{+/-}/SCID^{+/+} mouse liver. Three weeks after transplantation,

tumor formation was observed in the recipient liver (Fig. 5A). Double FISH analysis showed that the nuclei in the tumor cells hybridized with human probes, but not with mouse probes (Fig. 5B), indicating that the tumor is derived from monkey ES cells. Importantly, we did not detect any nuclei hybridized with both human and mouse DNA probes after monkey ES cell transplantation. These results clearly show that the differentiated monkey EB cells rather than contaminating undifferentiated monkey ES cells generate the hybrid hepatocytes by cell fusion in the uPA^{+/-}/SCID^{+/+} mouse liver.

Discussion

Since the characteristics of human ES cells are different from those of mouse ES cells, data obtained from mouse ES cells are partially applicable to research using human ES cells. The phenotype of monkey ES cells is known to be similar to that of human ES cells (Suemori et al. 2001). In the present study, we formed EBs from monkey ES cells and examined the expression of hepatocyte-related genes. We found that expression of many hepatocyte-related genes including Alb, Afp, Otc, and Cps1 in the developing monkey EBs. We have recently reported that Cyp7a1 gene is exclusively expressed in adult hepatocytes but not in visceral endoderm of yolk sac tissues in mice, and that its expression is induced in developing mouse EBs (Asahina et al. 2004). The Cyp7a1 expression was also detected in cultured monkey EBs. In addition, Cyp3a, which encodes a major drug-metabolizing enzyme in the liver, was expressed in developing monkey EBs, and its expression was induced by rifampicin. Double

immunocytochemistry showed that cells expressing both ALB and CK8/18 and both AAT and CK8/18 were present in the developing EBs, suggesting that functional hepatocytes are differentiated in the cultured monkey EBs.

We examined the effect of cytokines and extracellular matrices on the hepatic differentiation of cultured EBs. When HGF, FGF-1, FGF-2, FGF-4, SCF, and LIF were added singly or in combination to the culture medium of the EBs on non-coated dishes, no significant effect on the expression of Alb mRNA was observed (data not shown). In addition, extracellular matrices including gelatin, type I collagen, fibronectin, and Matrigel did not affect the expression of Alb mRNA in cultured EBs. We assume that hepatic differentiation proceeds in the presence of cytokines and extracellular matrices secreted from other cells in the developing EBs and presumably via cell-cell interactions under our culture condition. Dissociation of EBs may lead to efficient exposure of exogenous cytokines and hepatic differentiation of ES cell-derived cells in vitro.

Previously, we enriched mouse ES-derived hepatocytes by Percoll centrifugation because there were no specific antibodies for hepatocytes (Kumashiro et al. 2005). Although attempts have been made to purify ES-derived hepatocytes using Alb promoter, Alb is not specific for hepatocytes (Yamamoto et al. 2003; Asahina et al. 2004). In addition, transgenes were rapidly inactivated in developing ES cells. Thus, under the present situation, it is difficult to purify ES-derived hepatocytes in vitro. Therefore, we transplanted monkey EB cells without cell fractionation, and examined

the transplantability of ES-derived cells in uPA^{+/-}/SCID^{+/+} mouse liver.

The uPA mice were crossed with SCID mice and used as a xenogeneic transplantation model for human hepatocytes (Mercer et al. 2001; Tateno et al. 2004). The transgenic mice expressing uPA directed by Alb enhancer/promoter result in liver injury (Sandgren et al. 1991). Since the uPA transgene is frequently lost in the hemizygous uPA hepatocytes, transplanted hepatocytes as well as the transgene-deficient hepatocytes selectively repopulate in the recipient diseased liver (Sandgren et al. 1991; Rhim et al. 1994). It seems that the active proliferation of transplanted hepatocytes is attributed to the high production of HGF in injured liver region (Locaputo et al. 1999). Thus, uPA^{+/-}/SCID^{+/+} transgenic mice are used as a hepatocyte repopulation model rather than a liver disease model.

In the xenogeneic transplantation experiment, hepatocytes expressing monkey ALB were observed in the recipient mouse liver. In situ hybridization revealed that the average contribution of monkey-derived cells was about 19% in the red-colored nodules. Conversely, about 81% in the red-colored nodules were derived from the recovered recipient hepatocytes in the uPA^{+/-}/SCID^{+/+} livers. In the entire recipient liver, 7.4% of hepatocytes are derived from monkey cells. ELISA for human ALB revealed that the concentration of monkey ALB was 1.26 ± 0.24 $\mu\text{g/ml}$ in the mouse serum. The concentration of normal monkey serum was measured as 75.3 $\mu\text{g/ml}$ using this ELISA kit. The sensitivity of the ELISA for monkey ALB was about 100 times lower than that for human ALB. If the monkey ES cell-derived hepatocytes in the mouse liver are

functionally identical to normal monkey hepatocytes, we calculated that 1.7% of hepatocytes were derived from monkey cells in the recipient liver. The discrepancy between in situ hybridization analysis and ELISA suggests that monkey ES cell-derived hepatocytes are not fully functional in the recipient liver.

Three weeks after transplantation, no tumor formation was observed in all recipient mouse livers transplanted with day 21 EB cells. RT-PCR revealed that the expression of Oct-3/4, an ES cell marker, is low in day 21 EBs. We assume that a small number of ES cells in EBs are incapable of producing teratoma in the recipient liver. Elimination of contaminating ES cells by cell fractionation or a suicide gene will be necessary to reduce the risk of teratoma formation (Schuldiner et al. 2003; Kumashiro et al. 2005).

It has been reported that transplanted mouse hepatoblast cell lines integrate and repopulate in $uPA^{+/-}/SCID^{+/+}$ mouse liver without cell fusion (Strick-Marchand et al. 2004). To determine whether the repopulating hepatocytes found in the present study result from integration of monkey ES cell-derived hepatocytes or cell fusion between monkey and mouse cells, we performed FISH analysis on the liver sections. We found that the repopulating hepatocytes arise from cell fusion between transplanted monkey cells and recipient mouse hepatocytes. Hepatocyte colonies containing nuclei hybridized with only human probes were not detected in the recipient liver. The hybrid hepatocytes between monkey and mouse synthesize monkey ALB in the mouse liver, suggesting that monkey cells adopt as functional hepatocytes in the mouse liver. It is likely that the hybrid hepatocytes clonally repopulate as red-colored nodules in the

recipient mice. Hybrid hepatocytes between transplanted monkey cells and recipient mouse hepatocytes carrying the uPA gene might be injured by the uPA transgene.

Therefore, we assume that the cell fusion occurs between transplanted monkey cells and the recovered recipient hepatocytes.

Mouse undifferentiated ES cells fuse with mouse bone marrow cells and neural stem cells in vitro (Terada et al. 2002; Ying et al. 2002). In our experiments, no repopulating hepatocytes were observed in the uPA^{+/-}/SCID^{+/+} mouse liver after transplantation of the undifferentiated monkey ES cells. As observed in Fig. 5, ES cell transplantation resulted in the tumor formation in the mouse liver. FISH analysis showed that the origin of the tumor was monkey ES cells, and no tumor derived from cell fusion between monkey and mouse cells was observed. These results clearly show that the differentiated cells from monkey ES cells rather than contaminating undifferentiated monkey ES cells generate the hybrid hepatocytes by cell fusion in the uPA^{+/-}/SCID^{+/+} mouse liver.

Our study showed the hepatic commitment of monkey ES cells in vitro. It is unclear, however, whether about 5% of hepatocytes differentiated from monkey ES cells in vitro are responsible for the in vivo generation of hybrid hepatocytes, which occupy 7.4% in the entire liver. Grompe and colleagues (Wang et al. 2003; Willenbring et al. 2004) reported that bone marrow cells adopt hepatocyte phenotypes by cell fusion in fumarylacetoacetate hydrolase (FAH) deficiency mouse liver. They indicated that hematopoietic cells such as macrophages generate functional hepatocytes by cell fusion

in vivo, and that adult hepatocytes integrate into FAH deficiency mouse liver without cell fusion (Willenbring et al. 2004). Further studies will be required to determine whether monkey ES-derived hepatocytes fuse with host hepatocytes or repopulate without cell fusion in the liver. Nonetheless, it should be emphasized that hybrid hepatocytes generated by cell fusion between monkey EB cells and mouse hepatocytes are functional. Liver contains polyploid hepatocytes, the population of which increases during liver growth (Sigal et al. 1995). It seems likely that polyploidation of hepatocytes is associated with terminal differentiation and cell senescence. Our results suggest that liver is a permissive organ to survive and proliferate hybrid hepatocytes that generated by cell fusion. Cell fusion-based cell replacement therapy might be an alternative treatment for liver injury.

Acknowledgments

We thank F. Ono (Laboratory Primates, Tsukuba) for providing cynomolgus liver tissues and T. Irie, S. Kakinuma, Y. Kumashiro (Tokyo Medical and Dental University), Y. Kageyama, H. Kono and Y. Yoshizane (Yoshizato Project, CLUSTER, Hiroshima) for their advice and helpful discussion. This work was supported by Grants-in-Aid for Scientific Research (13470232, 15659067, 16390357, 17770051) from the Ministry of Education, Culture, Sports, Science and Technology of Japan, and by the Atsuko Ohuchi Memorial Research Fund for Medical Research.

References

- Asahina K, Fujimori H, Shimizu-Saito K, Kumashiro Y, Okamura K, Tanaka Y, Teramoto K, Arii S, Teraoka H (2004) Expression of the liver-specific gene Cyp7a1 reveals hepatic differentiation in embryoid bodies derived from mouse embryonic stem cells. *Genes Cells* 9:1297-1308
- Brandon EFA, Raap CD, Meijerman I, Beijnen JH, Schellens JHM (2003) An update on in vitro test methods in human hepatic drug biotransformation research: pros and cons. *Toxicol Appl Pharmacol* 189:233-246
- Chinzei R, Tanaka Y, Shimizu-Saito K, Hara Y, Kakinuma S, Watanabe M, Teramoto K, Arii S, Takase K, Sato C, Terada N, Teraoka H (2002) Embryoid-body cells derived from a mouse embryonic stem cell line show differentiation into functional hepatocytes. *Hepatology* 36:22-29
- Dandri M, Burda MR, Török E, Pollok JM, Iwanska A, Sommer G, Rogiers X, Rogler CE, Gupta S, Will H, Greten H, Petersen J (2001) Repopulation of mouse liver with human hepatocytes and in vivo infection with hepatitis B virus. *Hepatology* 33:981-988
- Doetschman TC, Eistetter H, Katz M, Schmidt W, Kemler R (1985) The in vitro development of blastocyst-derived embryonic stem cell lines: formation of visceral yolk sac, blood islands and myocardium. *J Embryol Exp Morphol* 87:27-45
- Evans MJ, Kaufman MH (1981) Establishment in culture of pluripotential cells from mouse embryos. *Nature* 292:154-156

- Ginis I, Luo Y, Miura T, Thies S, Brandenberger R, Gerecht-Nir S, Amit M, Hoke A, Carpenter MK, Itskovitz-Eldor J, Rao MS (2004) Differences between human and mouse embryonic stem cells. *Dev Biol* 269:360-380
- Hamazaki T, Iiboshi Y, Oka M, Papst PJ, Meacham AM, Zon LI, Terada N (2001) Hepatic maturation in differentiating embryonic stem cells in vitro. *FEBS Lett* 497:15-19
- Itskovitz-Eldor J, Schuldiner M, Karsenti D, Eden A, Yanuka O, Amit M, Soreq H, Benvenisty N (2000) Differentiation of human embryonic stem cells into embryoid bodies compromising the three embryonic germ layers. *Mol Med* 6:88-95
- Jochheim A, Hillemann T, Kania G, Scharf J, Attaran M, Manns MP, Wobus AM, Ott M (2004) Quantitative gene expression profiling reveals a fetal hepatic phenotype of murine ES-derived hepatocytes. *Int J Dev Biol* 48:23-29
- Jones EA, Tosh D, Wilson DI, Lindsay S, Forrester LM (2002) Hepatic differentiation of murine embryonic stem cells. *Exp Cell Res* 272:15-22
- Kumashiro Y, Asahina K, Ozeki R, Shimizu-Saito K, Tanaka Y, Kida Y, Inoue K, Kaneko M, Sato T, Teramoto K, Arai S, Teraoka H (2005) Enrichment of hepatocytes differentiated from mouse embryonic stem cells as a transplantable source. *Transplantation* 79:550-557
- Lavon N, Yanuka O, Benvenisty N (2004) Differentiation and isolation of hepatic-like cells from human embryonic stem cells. *Differentiation* 72:230-238
- Locaputo S, Carrick TL, Bezerra JA (1999) Zonal regulation of gene expression during

- liver regeneration of urokinase transgenic mice. *Hepatology* 29:1106-1113
- Martin GR (1981) Isolation of a pluripotent cell line from early mouse embryos cultured in medium conditioned by teratocarcinoma stem cells. *Proc Natl Acad Sci USA* 78:7634-7638
- Mercer DF, Schiller DE, Elliott JF, Douglas DN, Hao C, Rinfret A, Addison WR, Fischer KP, Churchill TA, Lakey JR, Tyrrell DL, Kneteman NM (2001) Hepatitis C virus replication in mice with chimeric human livers. *Nat Med* 7:927-933
- Ohashi K, Park F, Kay MA (2001) Hepatocyte transplantation: clinical and experimental application. *J Mol Med* 79:617-630
- Rae JM, Johnson MD, Lippman ME, Flockhart DA (2001) Rifampin is a selective, pleiotropic inducer of drug metabolism genes in human hepatocytes: studies with cDNA and oligonucleotide expression arrays. *J Pharmacol Exp Ther* 299:849-857
- Rambhatla L, Chiu CP, Kundu P, Peng Y, Carpenter MK (2003) Generation of hepatocyte-like cells from human embryonic stem cells. *Cell Transplant* 12:1-11
- Reubinoff BE, Pera MF, Fong CY, Trounson A, Bongso A (2000) Embryonic stem cell lines from human blastocysts: somatic differentiation in vitro. *Nat Biotechnol* 18:399-404
- Rhim JA, Sandgren EP, Degen JL, Palmiter RD, Brinster RL (1994) Replacement of diseased mouse liver by hepatic cell transplantation. *Science* 263:1149-1152
- Rhim JA, Sandgren EP, Palmiter RD, Brinster RL (1995) Complete reconstitution of mouse liver with xenogeneic hepatocytes. *Proc Natl Acad Sci USA* 92:4942-4946

Sandgren EP, Palmiter RD, Heckel JL, Daugherty CC, Brinster RL, Degen JL (1991)

Complete hepatic regeneration after somatic deletion of an albumin-plasminogen activator transgene. *Cell* 66:245-256

Schuldiner M, Itskovitz-Eldor J, Benvenisty N (2003) Selective ablation of human

embryonic stem cells expressing a “suicide” gene. *Stem Cells* 21:257-265

Sigal SH, Gupta S, Gebhard DF Jr, Holst P, Neufeld D, Reid LM (1995) Evidence for a

terminal differentiation process in the rat liver. *Differentiation* 59:35-42

Strain AJ, Neuberger JM (2002) A bioartificial liver-state of the art. *Science*

295:1005-1009

Strick-Marchand H, Morosan S, Charneau P, Kremsdorf D, Weiss MC (2004)

Bipotential mouse embryonic liver stem cell lines contribute to liver regeneration and differentiate as bile ducts and hepatocytes. *Proc Natl Acad Sci USA*

101:8360-8365

Suemori H, Tada T, Torii R, Hosoi Y, Kobayashi K, Imahie H, Kondo Y, Iritani A,

Nakatsuji N (2001) Establishment of embryonic stem cell lines from cynomolgus monkey blastocysts produced by IVF or ICSI. *Dev Dyn* 222:273-279

Tateno C, Yoshizane Y, Saito N, Kataoka M, Utoh R, Yamasaki C, Tachibana A, Soeno

Y, Asahina K, Hino H, Asahara T, Yokoi T, Furukawa T, Yoshizato K (2004) Near completely humanized liver in mice shows human-type metabolic responses to

drugs. *Am J Pathol* 165:901-912

Terada N, Hamazaki T, Oka M, Hoki M, Mastalerz DM, Nakano Y, Meyer EM, Morel L,

- Petersen BE, Scott EW (2002) Bone marrow cells adopt the phenotype of other cells by spontaneous cell fusion. *Nature* 416:542-545
- Thomson JA, Itskovitz-Eldor J, Shapiro SS, Waknitz MA, Swiergiel JJ, Marshall VS, Jones JM (1998) Embryonic stem cell lines derived from human blastocysts. *Science* 282:1145-1147
- Wang X, Willenbring H, Akkari Y, Torimaru Y, Foster M, Al-Dhalimy M, Lagasse E, Finegold M, Olson S, Grompe M (2003) Cell fusion is the principal source of bone-marrow-derived hepatocytes. *Nature* 422:897-901
- Willenbring H, Bailey AS, Foster M, Akkari Y, Dorrell C, Olson S, Finegold M, Fleming WH, Grompe M (2004) Myelomonocytic cells are sufficient for therapeutic cell fusion in liver. *Nat Med* 10:744-748
- Yamada T, Yoshikawa M, Kanda S, Kato Y, Nakajima Y, Ishizaka S, Tsunoda Y (2002) In vitro differentiation of embryonic stem cells into hepatocyte-like cells identified by cellular uptake of indocyanine green. *Stem Cells* 20:146-154
- Yamamoto H, Quinn G, Asari A, Yamanokuchi H, Teratani T, Terada M, Ochiya T (2003) Differentiation of embryonic stem cells into hepatocytes: biological functions and therapeutic application. *Hepatology* 37:983-993
- Ying QL, Nichols J, Evans EP, Smith AG (2002) Changing potency by spontaneous fusion. *Nature* 416:545-548

Figure legends

Fig. 1 Expression of hepatocyte-related genes in developing monkey EBs. (A) EBs were formed from monkey ES cells and cultured on non-coated dishes in the differentiation medium without exogenous cytokines. RNA samples were prepared from ES cells and differentiating EBs at day 3, 7, 14, and 21. The expression of Alb, Afp, Otc, Cps1, Cyp7a1, Oct-3/4, and β -actin mRNAs was determined by RT-PCR. Adult cynomolgus monkey liver (L) was used as a positive control. No amplification was detected in a negative control in which the mRNA was not treated with reverse transcriptase (RT-). (B) Quantitative analysis of Cyp3a expression. ES cells and EBs at culture day 25 were treated with 50 μ M rifampicin for 48 h. RNA samples were prepared, and the expressions of Cyp3a and β -actin mRNAs were determined by quantitative real-time RT-PCR. Cyp3a expression was up-regulated by rifampicin in EBs. The expression of Cyp3a in each sample was normalized according to the expression of β -actin in each sample. No expression was detected in undifferentiated ES cells. Values are the mean \pm SD of triplicate experiments.

Fig. 2 Immunocytochemistry of hepatic markers in developing monkey EBs. EBs were cultured on non-coated dishes for 21 days. (A) Developing EBs. (B,C) Fluorescent images of the same field shown in (A). ALB-positive cells (B, red) and CK8/18-positive cells (C, green) were seen in the developing EBs. (D) A merged image of the squares in (B) and (C). Cells positive for both antibodies to ALB and CK8/18 were seen

(arrowheads). Nuclei were visualized with DAPI staining (blue). (E) Without anti-ALB antibodies. (F) AAT-positive cells (red). (G) CK8/18-positive cells (green). (H) A merged image of (F) and (G). Cells positive for both AAT and CK8/18 antibodies were seen (arrowheads) in the developing EBs. Scale bar, (A-C, E) 60 μm ; (D, F-H) 20 μm .

Fig. 3 Xenogeneic cell transplantation of monkey EB cells in mouse liver.

Disaggregated cells from day 21 EBs were transplanted into $\text{uPA}^{+/-}/\text{SCID}^{+/+}$ mice that are immunodeficient and undergo liver failure. Three weeks after transplantation, the donor monkey cells were detected by genomic in situ hybridization and immunohistochemistry. (A) Two-week-old $\text{uPA}^{+/-}/\text{SCID}^{+/+}$ mouse liver without cell transplantation. $\text{uPA}^{+/-}/\text{SCID}^{+/+}$ liver is white-colored due to hepatic injury, and the transgene-deficient hepatocytes are seen as red foci (arrows). (B) $\text{uPA}^{+/-}/\text{SCID}^{+/+}$ mouse liver (Exp. 1, #1) three weeks after transplantation of monkey EB cells. Red nodules possibly derived from transgene-deficient recipient hepatocytes and/or transplanted monkey cells are seen (arrows). The proportion of red-colored nodules in the recipient liver is 46.5% (see Table 2). (C, D) Genomic in situ hybridization of human DNA probes. The nuclei of 43% cells on the monkey liver were positive for the human DNA probes (C). No signals were detected on $\text{uPA}^{+/-}/\text{SCID}^{+/+}$ mouse liver (D). (E, F) Immunohistochemistry of anti-human specific ALB antibodies on monkey (E) and $\text{uPA}^{+/-}/\text{SCID}^{+/+}$ mouse (F) liver sections. Monkey hepatocytes (E), but not $\text{uPA}^{+/-}/\text{SCID}^{+/+}$ mouse hepatocytes (F) were positive for the anti-human specific ALB

antibodies (red). (G) In situ hybridization of the human DNA probes on the red nodules in the $uPA^{+/-}/SCID^{+/+}$ mouse liver transplanted with monkey EB cells. Monkey EB-derived cells were detected in the recipient mouse liver (left side, arrows). (H) Immunohistochemistry of ALB on the section (G). The donor monkey cells (left side), but not recipient mouse hepatocytes (right side) were positive for ALB antibodies. Dashed lines in (G) and (H) indicate the boundary between repopulating monkey EB-derived cells and recipient mouse parenchyma. (I) Enlargement of the liver section (G). Clusters consisting of monkey EB-derived cells were detected in the recipient mouse liver (arrows). The nuclei of the monkey cells (I) were larger than those of the normal monkey hepatocytes (C). (J) Immunohistochemistry of ALB on the section (I). The donor monkey cells were positive for ALB antibodies (arrows). Scale bar, 30 μ m.

Fig. 4 Double FISH analysis on $uPA^{+/-}/SCID^{+/+}$ mouse liver transplanted with monkey EB cells. (A, B) Double FISH analysis of human DNA and mouse pan-centromeric probes on normal monkey liver. The nuclei of the monkey liver were hybridized with the human DNA probes (A, red), but not with the mouse DNA probes (B). (C, D) Double FISH analysis of human DNA and mouse pan-centromeric probes on control $uPA^{+/-}/SCID^{+/+}$ mouse liver. The human DNA probes did not hybridized with the mouse nuclei (C). The mouse DNA probes hybridized with mouse nuclei (D, green dots). The inset shows the enlargement of the nuclei in (D). (E-J) Double FISH analysis on the $uPA^{+/-}/SCID^{+/+}$ mouse liver transplanted with monkey EB cells. (E) The human DNA

probes (arrowheads, red). (F) The mouse DNA probes (arrowheads, green dots). (G) A merged image of (E) and (F). Nuclei hybridized with both human and mouse DNA probes were observed (arrowheads) in the uPA^{+/-}/SCID^{+/+} mouse liver. (H) Enlargement of (G). The large nuclei positive for both human and mouse DNA probes. (I, J) The recipient uPA^{+/-}/SCID^{+/+} mouse region of the same section (E). The recipient mouse hepatocytes were positive for the mouse DNA probes (J), but not for the human DNA probes (I). Scale bar, 20 μ m.

Fig. 5 Tumor formation in the uPA^{+/-}/SCID^{+/+} mouse liver after undifferentiated monkey ES cell transplantation. (A) Hematoxylin and eosin staining. Tumor formation was observed in the recipient mouse liver (right side). (B) Double FISH analysis on the section (A). The nuclei of the tumor were hybridized with the human DNA probes (red), but not with the mouse probes. The recipient mouse hepatocytes (left side) were hybridized with the mouse DNA probes (green dots), but not with the human probes. Scale bar, 20 μ m.

Table 1 Sequences of PCR primers

Gene	Primer		Cycles	Size (bp)
hAlb	Forward	5'-GATGTCTTCCTGGGCATGTT-3'	35	342
	Reverse	5'-ACATTTGCTGCCCACTTTTC-3'		
hAfp	Forward	5'-TGCCAACTCAGTGAGGACAA-3'	33	356
	Reverse	5'-TCCAACAGGCCTGAGAAATC-3'		
hOtc	Forward	5'-GAGTTTTCAAGGGCATAGAATCGTC-3'	33	209
	Reverse	5'-CAGATCTGCTGATAGCCAT-3'		
hCps1	Forward	5'-GCCATTGAAAAGGTGAAGGA-3'	33	481
	Reverse	5'-CAGCCACACCAAGGAATCTT-3'		
hCyp7a1	Forward	5'-AATTCATACCTGGGCTGTG-3'	35	383
	Reverse	5'-AGGCAGCGGTCTTTGAGTTA-3'		
hOct-3/4	Forward	5'-AGGTGTGGGGGATTCCCCCAT-3'	30	625
	Reverse	5'-GCGATGTGGCTGATCTGCTGC-3'		
hβ-actin	Forward	5'-GGACTTCGAGCAAGAGATGG-3'	25	404
	Reverse	5'-ACATCTGCTGGAAGGTGGAC-3'		
cyAlb	Forward	5'-GCATCCTGATTACTCTGACATG-3'	35	229
	Reverse	5'-CTTGGTGTAACGAACTAATTGC-3'		
cyAfp	Forward	5'-GGGAGCGGCTGACATTATTA-3'	33	232
	Reverse	5'-CACCTGAGCTTGACACAGA-3'		
cyOtc	Forward	5'-GAGGATCCTGTTGAACAATGC-3'	32	103
	Reverse	5'-GCCCTTCAGCTGCACTTTAT-3'		
cyCps1	Forward	5'-GATCCTTCCCCTTTGTTTCC-3'	33	304
	Reverse	5'-AGGATGCCTTTCTGGGGTAT-3'		
cyCyp3a	Forward	5'-ATACACGCCCTTTGGAAGTG-3'	35	440
	Reverse	5'-TCCCCTGCACTAATTTGGTC-3'		

Gene	Primer		Cycles	Size (bp)
cyCyp7a1	Forward	5'-ATTTGGTGCCAATCCTCTTG-3'	35	312
	Reverse	5'-CGTTGGAGGTTTTCCATCAT-3'		
cyOct-3/4	Forward	5'-GAGGAGTCCCAGGACATCAA-3'	30	307
	Reverse	5'-CTGGTTCGCTTTCTCTTTTCG-3'		
cyβ-actin	Forward	5'-TCCCTGGAGAAGAGCTACGA-3'	25	243
	Reverse	5'-CTTCTGCATCCTGTCAGCAA-3'		

Table 2 Percentage of monkey-derived cells in the recipient mouse liver

Experiment	Mouse	Proportion of red-colored nodules in the recipient liver (%) ^a	Liver sample ^b	Percentage of monkey-derived cells in the red-colored nodules of the recipient liver	Percentage of monkey-derived cells in the entire recipient liver ^c
1	#1	46.5	Red	33.9	15.8
	#2	23.7	Red	16.2	3.8
	#3	27.1	Red	5.6	1.5
2	#1	23.9	Entire liver	–	9.0
	#2	22.6	Entire liver	–	13.6
	#3	ND	Entire liver	–	0.5
Average ± SD		28.8±9.0	–	18.6±11.7	7.4±5.9

ND not determined

^aThe proportion of the red-colored nodules was calculated as the ratio of the red-colored nodule area to the entire area of the liver

^bThe red-colored nodules were examined by genomic in-situ hybridization in Experiment 1, whereas the entire liver was examined in Experiment 2

^cIn Experiment 1, the percentage of monkey-derived cells in the entire liver was calculated from the proportion of the red-colored nodules in the recipient liver and the percentage of monkey-derived cells in the red-colored nodules of the liver

Fig. 1

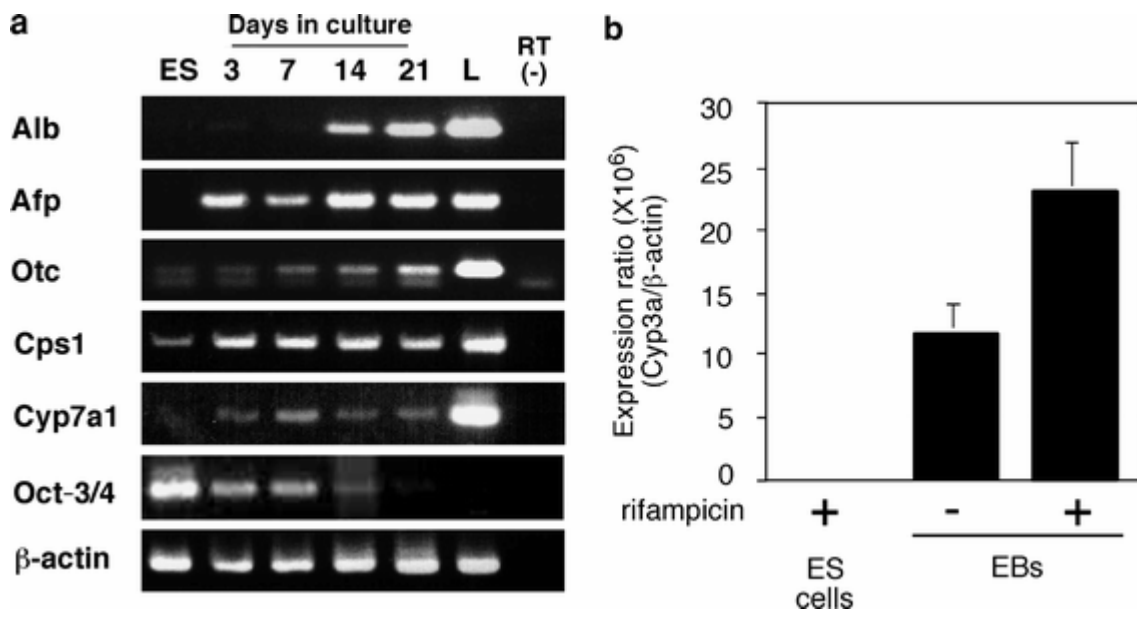


Fig. 2

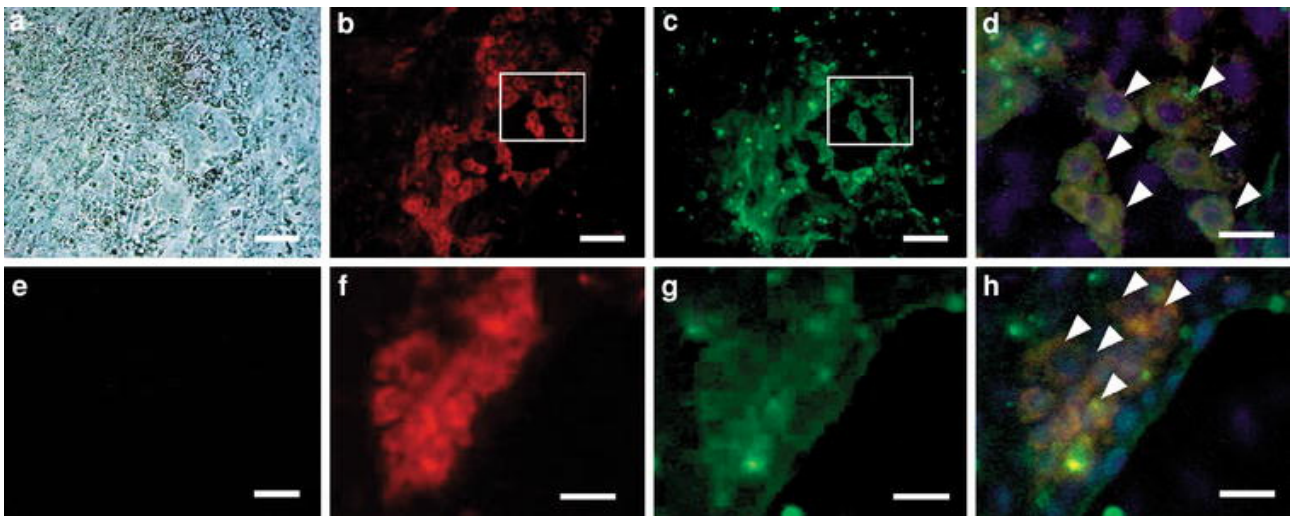


Fig. 3

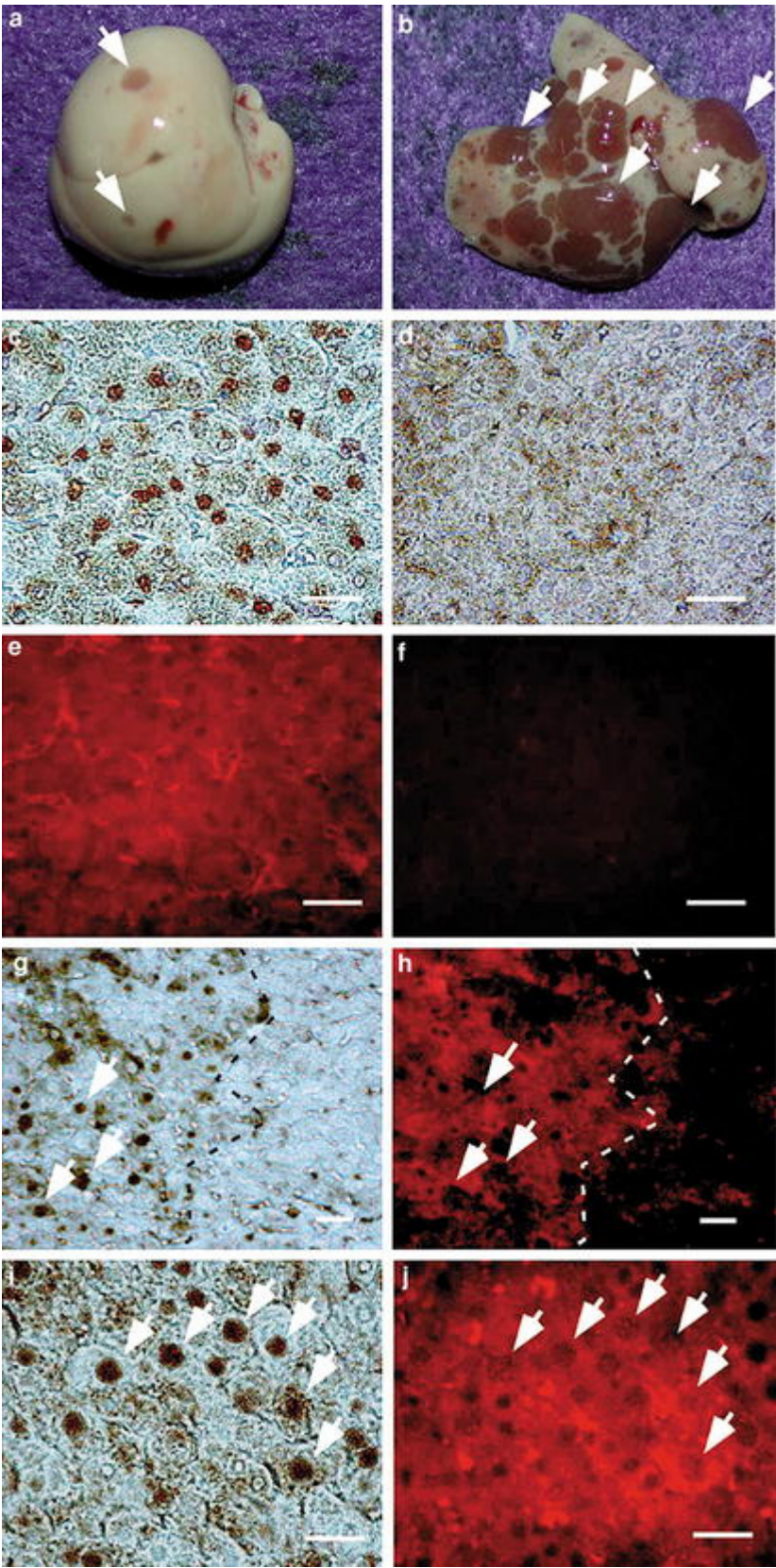


Fig. 4

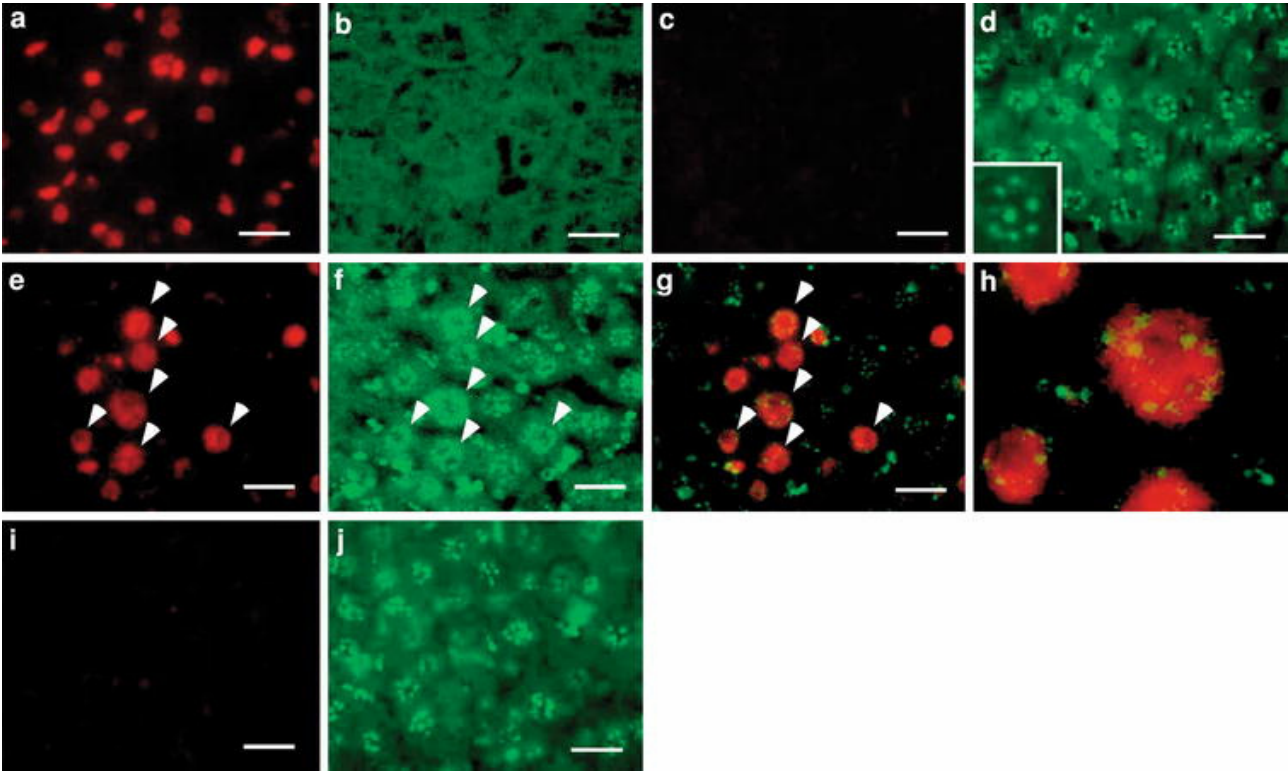


Fig. 5

